International Journal of Mass Spectrometry and Ion Processes, 77 (1987) 187–201
Elsevier Science Publishers B.V., Amsterdam – Printed in The Netherlands

AN AB INITIO STUDY OF THE ISOMERISATION AND FRAGMENTATION OF CHO_2^+ IONS: AN EXAMPLE OF SPIN-CONTROLLED REACTIONS?

F. REMACLE *, S. PETITJEAN **, D. DEHARENG and J.C. LORQUET ***
Département de Chimie, Université de Liège, Sart-Tilman, B-4000 Liège 1 (Belgium)
(First received 27 February 1987; in final form 14 May 1987)

ABSTRACT

[CHO_2^+] ions exist in two isomeric forms, a quasi-linear carboxylic structure, $OCOH^+$ (I), and a formate structure, $O(CH)O^+$ (II). The latter is known to isomerise into the former with a low rate constant (about 10^5 s^{-1}). Configuration interaction ab initio calculations reveal that the ion can exist in three low-lying electronic states of different multiplicity and symmetry species, a singlet ($\tilde{X}^1A'$) and two triplets ($\tilde{a}^3A'$ and $\tilde{b}^3A''$). The potential energy surfaces cross so that the nature of the lowest state varies as a function of the nuclear geometry. The singlet surface ($\tilde{X}^1A'$) has its deepest minimum for structure I and a subsidiary minimum for structure II. The situation is reversed for the $\tilde{a}^3A'$ state which has its deepest minimum for structure II and which exhibits a shallow minimum for structure I. Thus, at low energies, the carboxylic and formate ions are respectively in a singlet and in a triplet state. These ions lose an oxygen atom on a microsecond time scale by a composite mechanism which is subject to a large isotope effect. One of the components of the metastable peak corresponds to reaction

$$OCOH^+(^1A') \rightarrow O(CH)O^+(^3A') \rightarrow HCO^+ + O$$

giving rise to a small kinetic energy release. The second component is due to a spin–orbit controlled direct predissociation process, viz.

$$OCOH^+(^1A') \rightarrow OCOH^+(^3A') \rightarrow HOC^+ + O$$

The probability of surface hopping varies as a function of the internal energy between 0 and a maximum value of ca. 0.008. The corresponding kinetic energy release is expected to be larger for the deuterated than for the hydrogenated compound. Thus, the two components are resolved in the deuterated compound, but hardly distinguishable in the hydrogenated species.

---

* Aspirant du Fonds National Belge de la Recherche Scientifique.
** Boursier de l'I.R.S.I.A.
*** To whom correspondence should be addressed.

0168-1176/87/$03.50

INTRODUCTION

There has been much interest in ions of global structure [CHO_2^+], both from experimental [1] and theoretical [2–9] viewpoints. Several authors have calculated ab initio their equilibrium geometries and have detected two isomeric structures: the carboxylic $OCOH^+$ and the formate $O(CH)O^+$ cations. On the lowest singlet potential energy surface, the former structure appears as a deeper minimum than the latter [4,8,9]. However, the situation is reversed for the lowest triplet state. The $O(CH)O^+$ structure has been shown [5] to be more stable in the $^3A'$ than in the $^1A'$ state. Bursey et al. thus suggest that a correct discussion of the reactivity of the ions requires specification of the multiplicity of the reactant. This will be attempted in the present paper in which we wish to show that there exist two groups of experimental data which indicate that the behaviour of these ions involves interactions between singlet and triplet states.

Two research groups [5,10] have found the $O(CH)O^+$ isomer to rearrange spontaneously into the carboxylic structure $OCOH^+$ with a rate constant of about 10^5 s^{-1}. Such a low value is certainly compatible with a singlet–triplet isomerisation process. In addition, there exists another set of puzzling measurements whose interpretation leads to the same conclusion. Burgers et al. [11] have observed a metastable fragmentation of the [CXO_2^+] ions (X = H or D) which apparently takes place in a different way in each isotope. The peak shape is clearly composite (with an important dished component) for the deuterated compound, whereas it is apparently simply Gaussian for the hydrogenated species. These authors suggest the schemes

$$OCOD^+ \rightarrow DOC^+ + O \tag{1}$$

characterised by a large kinetic energy release ($T_{0.5} \simeq 180$ meV), and

$$OCOD^+ \rightarrow O(CD)O^+ \rightarrow DCO^+ + O \tag{2}$$

with a much smaller kinetic energy release ($T_{0.5} \simeq 45$ meV).

According to the authors' published interpretation, the unusual isotope effect on the peak shape is due to the fact that only channel (2) is open for the hydrogenated species in the time scale of metastable transitions. Now, the Wigner–Witmer correlation rules [12] indicate that production of an oxygen atom in its triplet ground state plus another fragment in a singlet state necessarily implies that the fragmentation process takes place on a triplet potential energy surface. If, as is highly probable, reactions (1) and (2) involve the lowest state of the reactant, i.e. the $OCOX^+$ structure in a singlet state, then, necessarily, reactions (1) and (2) require a surface hopping between singlet and triplet states.

The purpose of the present paper is to get a *qualitative* knowledge of the potential energy surfaces of the lowest electronic states and to identify the molecular processes which control reactions (1) and (2). For reasons just discussed, particular attention has to be paid to the lowest $^1A'$, $^3A'$, and $^3A''$ states and to the spin–orbit interaction which exists between them.

COMPUTATIONAL METHODS

High-quality determinations of the *structural* properties of the ion are available [2–9], but very little exists for a study of its *dynamical* properties. In the latter case, constructing diagrams which represent the potential energy surface of the ground state as a succession of equilibrium structures separated by transition states, all this plotted along a succession of ill-defined reaction coordinates, is not the appropriate strategy for two reasons. First, in problems in which several electronic states are expected to be involved, the use of configuration interaction (CI) wave functions offers great advantages over the SCF approximation [13]. Secondly, our aim is to inject later on the results of the qualitative analysis which is presented here into a statistical expression of the rate constants. In this theory [14,15], a partition is made between a set of (usually just two) crucial degrees of freedom (including, of course, the reaction coordinate), and the remaining set of "spectator" degrees of freedom which play a much less important role. The necessary information has to be found in two-dimensional graphs of a set of potential energy surfaces extending over a rather large range of the nuclear configuration space and this for several electronic states. For practical reasons, this inevitably implies restricting the size of the basis set of atomic orbitals, at least in a preliminary study.

Configuration interaction calculations have therefore been carried out using a standard Dunning basis set of atomic orbitals (AOs) [16]. For carbon and oxygen, we use the $[3s2p]$ contraction of the Huzinaga $[9s5p]$ set. For hydrogen, we use the $[2s]$ contraction of the $[4s]$ set, multiplied by a scale factor of 1.2. This is a split valence-shell basis, without polarization AOs. As a result, quantitative accuracy cannot be expected for the energy gaps and barriers derived from the calculations. For each state, the CI wave function has been expanded in a set of configuration state functions (CSFs) which were generated from two reference configurations. All the singly-excited plus part of the doubly-excited configurations have been included in the expansion. The molecular orbitals (MOs), among which the double excitations were allowed, ranged from $4a'$ to $13a'$ and from $1a''$ to $4a''$ in the case of the singlet matrix. For both triplet states, the range was restricted to $(4a'–11a')$ and to $(1a''–4a'')$.

For the $^1A'$ state, the reference configurations are

$$\Phi_1 = \ldots(9a')^2(10a')^2(1a'')^2$$

$$\Phi_2 = \ldots(9a')^2(1a'')^2(2a'')^2$$

and the expansion included 1292 CSFs.

For the $^3A'$ state, the reference configurations are

$$\Phi_3 = \ldots(9a')^2(2a'')^1(3a'')^1$$

$$\Phi_4 = \ldots(9a')^1(10a')^1(2a'')^2$$

and 1692 CSFs were generated.

The reference configurations of the $^3A''$ state are

$$\Phi_5 = \ldots(9a')^2(10a')^1(2a'')^1$$

$$\Phi_6 = \ldots(9a')^1(2a'')^2(3a'')^1$$

The size of the CI matrix is equal to 1705.

The ALCHEMY–MOLECULE system of programs [17] was used throughout.

In order to obtain a simple graphical representation, the surfaces have to be plotted as a function of two coordinates only [Fig. 1]. Therefore, only planar geometries have been considered. One of the CO bond distances has been frozen to a value of 1.246 Å (i.e. to the equilibrium value calculated by Seeger et al. [4]). Two sets of calculations were then carried out.

(1) A first set was used to determine the general features and the ordering of the lowest potential energy surfaces. These calculations, reported in the next section, lead to an interpretation of the isomerisation reaction. For that purpose, remaining coordinates have been defined with respect to the centre

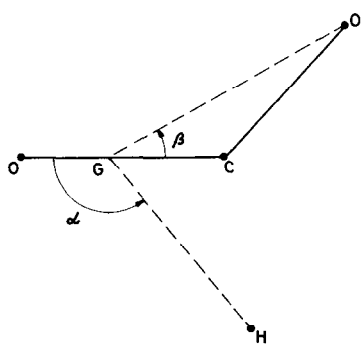

Fig. 1. Geometry of the [CHO_2^+] ion in the system of coordinates (α, β).

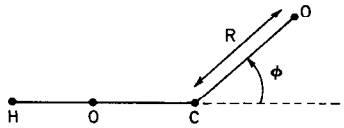

Fig. 2. Geometry of the $HOCO^+$ ion in the system of coordinates (R, ϕ).

of mass, G, of the fixed CO bond. The distances GH and GO (between G and the mobile atoms) have been frozen to values of 1.5 Å and 1.8 Å, respectively (inspired by the results of previous calculations [4,5]). The potential energy surfaces have been plotted as a function of the angles α and β defined in Fig. 1. A value of α close to 0° corresponds to the linear $HOCO^+$ structure, whereas the other isomer $O(CH)O^+$ implies $\alpha \simeq 140°$.

For these calculations, the method of the intermediate configuration has been adopted [18–20]: the same MOs have been calculated for the three states $^1A'$, $^3A'$, and $^3A''$. These MOs are eigenfunctions of a unique Hamiltonian corresponding to the fictitious configuration $(9a')^2(10a')^{1/2}(2a'')^2(3a'')^{1/2}$, in which all the MOs which appear in the reference configurations Φ_1 to Φ_6 are occupied.

As a result of these calculations, localised regions of non-adiabatic interaction will be recognised, and reasonable reaction mechanisms will emerge.

(2) Since the previous calculations led to the conclusion that for a non-adiabatic reaction the optimum value of α is equal to zero, a second series of calculations was then attempted. The potential energy surfaces are now plotted as a function of two coordinates (R, ϕ) defined in Fig. 2. Coordinate R measures the extension of the breaking CO bond length and ϕ is a polar angle. The fixed CO and OH bond distances were frozen to values of 1.246 and 0.969 Å, respectively. The corresponding potential energy surfaces reveal that at least one of the metastable fragmentations (viz. that leading to the production of the HOC^+) results from an electronic predissociation process.

THE ISOMERISATION PROCESS

Energy contours for the three states $^1A'$, $^3A'$, and $^3A''$, are represented in Figs. 3–5. The three surfaces are found to cross along loci of intersection (the "seams") which are also represented in these figures.

The lowest states are the $^1A'$ and $^3A'$. The $^3A''$ state is found to lie nearly always at a higher energy than the other two. Careful inspection of the surfaces (together with additional calculations not reported here) reveals that the $^3A''$ state does not play a role in the threshold mechanisms leading

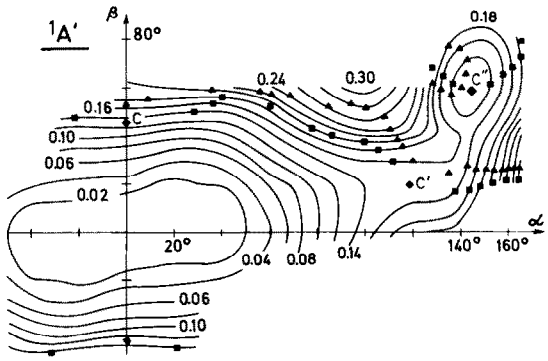

Fig. 3. Energy contours of the $\tilde{X}^1A'$ state plotted as a function of the coordinates α and β. The contour interval is 0.02 u (1 a.u. = 27.21 eV). The energies are measured from the energy minimum of the state $\tilde{X}^1A'$. Squares and triangles represent, respectively, the seam between the $\tilde{X}^1A'$ and the $\tilde{a}^3A'$ states and the seam between the $\tilde{X}^1A'$ and the $\tilde{b}^3A''$ states. Diamonds represent the lowest energy crossing points between the $\tilde{X}^1A'$ and the $\tilde{a}^3A'$ states (points C, C′, C″).

to isomerisation and fragmentation into HOC^+. However, the $^3A''$ state might be involved in the final steps leading to the production of the fragment HCO^+. We shall therefore focus attention on the interaction between $^1A'$ and $^3A'$. A schematic view of their ordering is shown in Fig. 6.

Inspection of Figs. 3–5 reveals the following.

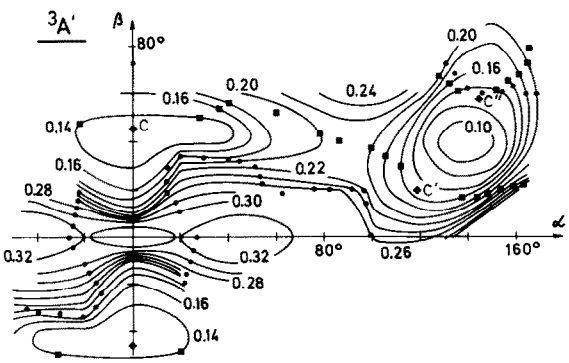

Fig. 4. Energy contours of the $\tilde{a}^3A'$ state plotted as a function of the coordinates α and β. The contour interval is 0.02 u. The energies are measured from the energy minimum of the state $\tilde{X}^1A'$. Squares and dots represent, respectively, the seam between the $\tilde{X}^1A'$ and the $\tilde{a}^3A'$ states and the seam between the $\tilde{a}^3A'$ and the $\tilde{b}^3A''$ states. Diamonds represent the lowest energy crossing points between the $\tilde{X}^1A'$ and the $\tilde{a}^3A'$ states (points C, C′, C″).

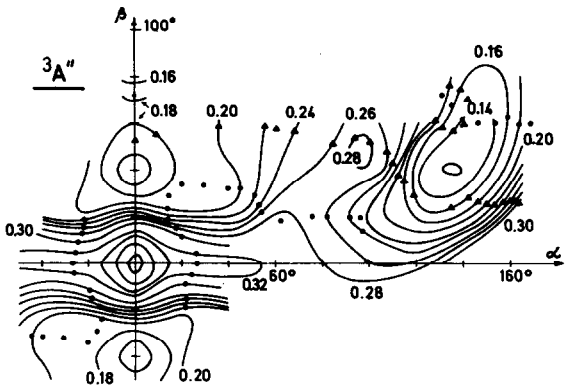

Fig. 5. Energy contours of the $\tilde{b}^3A''$ state plotted as a function of the coordinates α and β. The contour interval is 0.02 u. The energies are measured from the energy minimum of the state $\tilde{X}^1A'$. Triangles and dots represent, respectively, the seam between the $\tilde{X}^1A'$ and $\tilde{a}^3A''$ states and the seam between the $\tilde{a}^3A'$ and the $\tilde{b}^3A''$ states.

The $\tilde{X}^1A'$ state

This state has its deepest minimum around the $HOCO^+$ structure. However, large-amplitude motions both of the oxygen and of the hydrogen atoms are possible around the CO core, so that the ion is found to have a floppy structure, in conformity with previous studies [2–9]. A secondary minimum corresponding to the $O(CH)O^+$ structure $[(\alpha, \beta) \simeq (140°, 60°)]$ clearly shows up. Both minima are separated by a saddle point around $(\alpha, \beta) \simeq (120°, 20°)$. On the whole, there is good agreement with the SCF results of Seeger et al. [4].

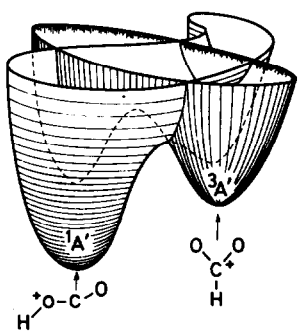

Fig. 6. Schematic view of the potential energy surfaces of the $\tilde{X}^1A'$ and $\tilde{a}^3A'$ states.

The $\tilde{a}^3A'$ state

This state exhibits its deepest minimum for the $O(CH)O^+$ structure, as already found by Bursey et al. [5] in their SCF STO 3G calculations [$(\alpha, \beta) \simeq (140°, 40°)$]. Two secondary minima corresponding to the $HOCO^+$ structure also exist. They are symmetrically located around points $(\alpha, \beta) = (20°, 40°)$ and $(-20°, -40°)$. These minima are separated by saddle-points at $(\alpha, \beta) = (90°, 40°)$ and $(\pm 20°, 0°)$.

The $\tilde{b}^3A''$ state

This state has also its deepest minimum at the $O(CH)O^+$ structure [$(\alpha, \beta) = (135°, 40°)$], and secondary minima at $(\alpha, \beta) = (0°, \pm 40°)$.

The seams

Of particular interest is the locus of intersection between the $\tilde{X}^1A'$ and $\tilde{a}^3A'$ states, which is represented by squares in Figs. 3 and 4. A perspective plot is presented in Fig. 7. The three points at which the intersystem crossing requires the least energy are represented by diamonds in these figures. The lowest energy crossing takes place at point C [$(\alpha, \beta) = (0°, 45°)$]. Two other possibilities exist at points C′ (120°, 20°) and C″ (140°, 60°).

Mechanisms of isomerisation

According to measurements carried out by Burgers et al. [10], the $O(CH)O^+$ ions isomerise to the $OCOH^+$ structure with a lifetime of the

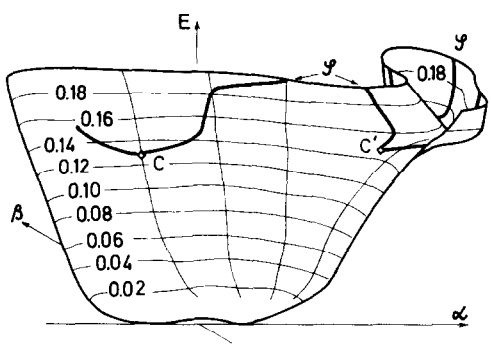

Fig. 7. Perspective plot of the seam between the $\tilde{X}^1A'$ and $\tilde{a}^3A'$ states. Diamonds represent the lowest energy crossing points between these states (points C′ and C″).

order of 10^{-5} s. As suggested by Bursey et al. [5], it is reasonable to think that the $O(CH)O^+$ ion reacts in its $^3A'$ state since (i) this corresponds to its most stable structure, and (ii) the ion is created by a collision-induced charge stripping from the anion, i.e. by a collision process which need not obey any multiplicity conservation rule. The slow isomerisation process thus corresponds to the spin-forbidden transition to the $HOCO^+$ ion in its $^1A'$ state. The most favourable crossing takes place at point C' [geometry $(\alpha, \beta) = (120°, 20°)$].

However, the spin-forbidden character of the transition alone is probably insufficient to account for the observed low rate of isomerisation. The process is probably slowed down by additional factors linked to the complicated shape of the potential energy surfaces.

THE METASTABLE FRAGMENTATION

On the basis of the previous results, two mechanisms can be proposed for the metastable loss of an oxygen atom. First, a spin–orbit controlled but otherwise direct dissociation, in which the reactant always retains the quasi-linear structure and which leads to the least stable isomer XOC^+.

$$XOCO^+(^1A') \rightarrow XOCO^+(^3A') \rightarrow XOC^+(^1\Sigma^+) + O(^3P) \qquad (1')$$

The singlet–triplet surface hopping takes place at point C [$(\alpha, \beta) = (0°, 45°)$].

Secondly, an indirect process, leading to the most stable fragment XCO^+ via the spin-forbidden isomerisation to the $O(CX)O^+$ structure discussed in the previous paragraph.

$$XOCO^+(^1A') \rightarrow O(CX)O^+(^3A') \rightarrow XCO^+(^1\Sigma^+) + O(^3P) \qquad (2')$$

This is in complete agreement with the mechanism proposed by Burgers et al. [11], except that there is no obvious explanation for the origin of the isotope effect. Reaction (2') accounts for the narrow Gaussian component which is not affected by isotope substitution. But why should reaction (1') contribute to the production of oxygen atoms in the metastable time scale for the deuterated compound only and not for the normal compound? Additional ab initio calculations were therefore carried out to obtain a more explicit picture of this particular reaction.

Potential energy surfaces

These surfaces, plotted as a function of coordinates R and ϕ are represented in Fig. 8 (for the $^1A'$ state) and Fig. 9 (for the $^3A'$ state). Also represented is the seam between both surfaces. The minimum energy of the

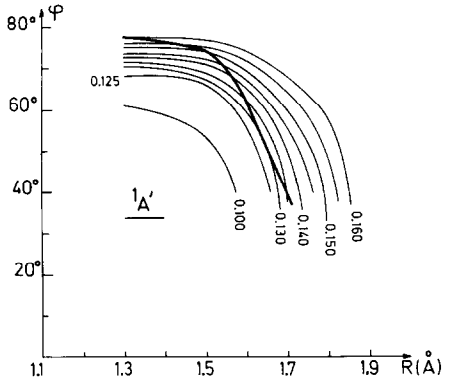

Fig. 8. Potential energy surface of the state $\tilde{X}^1A'$ plotted as a function of coordinates R and ϕ. The contour interval is 0.005 u. The energies are measured from the energy minimum of the state $\tilde{X}^1A'$. The thick line represents the seam between the $\tilde{X}^1A'$ and $\tilde{a}^3A'$ states.

locus of intersection is located at point $R = 1.65$ Å, $\phi = 50°$. A cross-section for the optimal value of the angle ϕ is given in Fig. 10. It represents, as a function of the reaction coordinate R, the non-adiabatic reaction path responsible for the metastable dissociation leading to the HOC^+ fragment. Clearly, one has to deal with a spin–orbit controlled predissociation.

Spin–orbit interaction

Spin–orbit coupling is an interaction which couples states of different multiplicities and allows radiationless transitions between, for example,

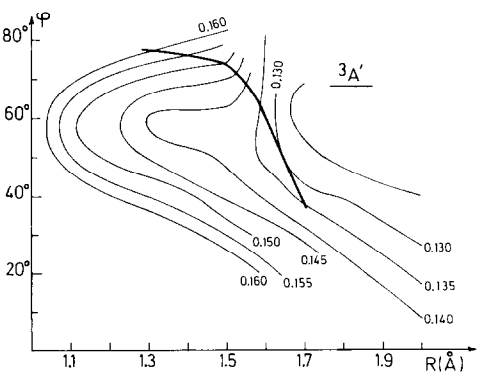

Fig. 9. Potential energy surface of the state $\tilde{a}^3A'$ plotted as a function of coordinates R and ϕ. The contour interval is 0.005 u. The energies are measured from the energy minimum of the state $\tilde{X}^1A'$. The thick line represents the seam between the $\tilde{X}^1A'$ and $\tilde{a}^3A'$ states.

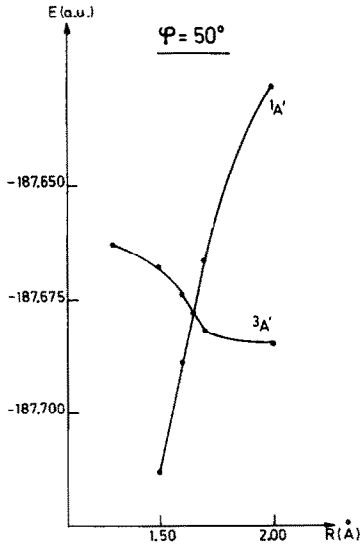

Fig. 10. Section of the potential energy surfaces of the states $\tilde{X}^1A'$ and $\tilde{a}^3A'$ plotted as a function of R ($\phi = 50°$).

singlet and triplet surfaces. According to time-dependent perturbation theory [21], the transition probability is proportional to the square of an off-diagonal matrix element

$$V_{SO} = \langle \Psi_T \mid H_{SO} \mid \Psi_S \rangle$$

in which Ψ_T and Ψ_S refer to the wave functions of the $\tilde{a}^3A'$ and $\tilde{X}^1A'$ states, respectively. Each of them is given by a CI expansion in CSFs. Since the spin–orbit coupling operator is given by a summation of one-electron operators [22], only the pairs of CSFs which differ by, at most, one spin orbital contribute to V_{SO}. Each MO is then expanded in the set of the AOs. Then, V_{SO} is given by a sum of terms [23], each of which is equal to a product of LCAO and CI coefficients multiplied by an elementary matrix element between AOs called ζ_{2p} [24]. The latter can be estimated from experimental spectroscopic data on atoms and elementary ions [25]. This leads to a value of about 40 cm^{-1} for V_{SO}.

Transition probability

The probability of undergoing a transition from the bound state $\tilde{X}^1A'$ to the repulsive $\tilde{a}^3A'$, i.e., the probability of undergoing a predissociation process (Fig. 10) can then be estimated from the simple Landau–Zener formula or from the much more accurate weak-coupling formula [26–28].

Both involve the value of V_{SO} (which has just been calculated) and the slopes of the two potential energy curves at the crossing point, which can be read off Fig. 10. One finds $F_S = 6.48$ eV Å^{-1} and $F_T = -1.95$ eV Å^{-1}. Also needed is the value, E_x, of the kinetic energy in the reaction coordinate. It is equal to the internal energy in the reaction coordinate (E_R) minus that of the crossing point (E_C).

$$E_x = E_R - E_C = (1/2)\mu v^2$$

The Landau–Zener formula becomes very inaccurate as $E_x \to 0$ and, in particular, is unable to account for tunneling [26–28]. Since it is precisely this energy range which is responsible for the metastable fragmentation, we have to abandon it in favour of the more accurate weak-coupling formula. The transition probabilities predicted by this equation exhibit an oscillatory character of quantum origin, as shown in Fig. 11. That part of the graph corresponding to negative values of E_x describes the tunnel effect. Also represented by broken lines is the Landau–Zener formula. The latter gives an average value at high energies only, but fails at lower energies.

The probability of undergoing a predissociation process is found to oscillate as a function of energy between values of zero and approximately 0.008. Too much attention should not be paid to these oscillations of quantum origin. At a given total internal energy, E, they will be washed out as a result of the integration over all the possible values in the reaction coordinate. Since there is no reason to express doubts about the fact that the ions react in a state of microcanonical equilibrium, what is now required is an extension of the QET–RRKM theory which would enable us to calculate rate constants for non-adiabatic processes. We are currently working on expressions in which the rate constant (just as in the usual RRKM/QET

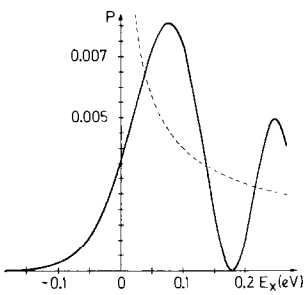

Fig. 11. Transition probability plotted as a function of E_X, the kinetic energy in the reaction coordinate. The broken line represents the Landau–Zener probability and the thick line represents the weak-coupling probability.

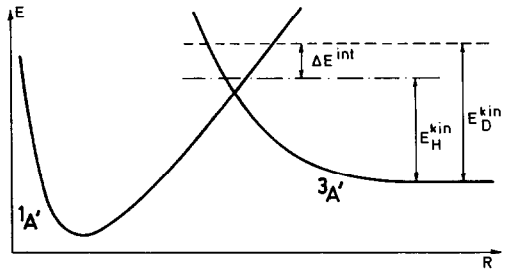

Fig. 12. Kinetic energy releases (E_H^{kin} and E_D^{kin}) for the dissociation of the $HOCO^+$ and $DOCO^+$ ions when the rate constant is equal to 10^6 s^{-1}.

equations) is given by a summation over the various exit channels, each one being weighted by the appropriate non-adiabatic transition probability.

A qualitative explanation of the isotope effect can already be put forward. In statistical models based on a state of microcanonical equilibrium, hydrogenated compounds are found to react faster than deuterated species. The reasons, which have been explained by Forst in the case of an adiabatic process [29], remain true for a non-adiabatic reaction [14,15]. Thus, the hydrogenated compound is expected to undergo predissociation in the metastable time scale at a lower internal energy than the deuterated compound. As a result, the kinetic energy release will be lower for the former than for the latter (Fig. 12). Thus, both dissociation processes (1) and (2) take place in competition in both isotopic molecules. However, for HCO_2^+, both reactions lead to similar (and relatively small) kinetic energy releases and thus to an apparently one-component simple Gaussian signal. On the other hand, for DCO_2^+ the kinetic energy release retains the same value for process (2) but is much larger for process (1). Hence the composite nature of the peak. Thus, if this interpretation is correct, the metastable fragmentation should also be composite in the hydrogenated species, i.e. both fragments HOC^+ and HCO^+ should be produced. In a private communication, we have been informed by Burgers et al. that this may indeed be the case. A quantitative estimate of the differences in the kinetic energy release of both species has to await the development of a theory of rate constants and kinetic shifts for non-adiabatic reactions. We will shortly report on this [14,15].

ACKNOWLEDGEMENTS

The authors are indebted to Professor P.C. Burgers and J.L. Holmes and to Dr. J.K. Terlouw for fruitful discussions and for carrying out the additional measurement on the isomeric composition of the metastable peak.

F.R. and S.P. thank, respectively, the F.N.R.S. and the I.R.S.I.A. for research fellowships. This work has been supported by the Belgian Government (programme d'Actions de Recherche Concertées) and by the Fonds de la Recherche Fondamentale Collective.

REFERENCES

1 T. Amano and K. Tanaka, J. Chem. Phys., 82 (1985) 1045; 83 (1985) 3721. M. Bogey, C. Demuynck and J.L. Destombes, J. Chem. Phys., 84 (1986) 10.
2 S. Green, H. Schor, P. Siegbahn and P. Thaddeus, Chem. Phys., 17 (1976) 479.
3 P. Cremaschi and M. Simonetta, Theor. Chim. Acta, 34 (1974) 175.
4 U. Seeger, R. Seeger, J.A. Pople and P. v. R. Schleyer, Chem. Phys. Lett., 55 (1978) 399.
5 M.M. Bursey, D.J. Harvan, C.E. Parker, L.G. Pedersen and J.R. Hass, J. Am. Chem. Soc., 101 (1979) 5489.
6 J.R. Bews, C. Glidewell and P.H. Vidaud, J. Mol. Struct., 64 (1980) 75.
7 D.J. De Frees, G.H. Loew and A.D. McLean, Astrophys. J., 254 (1982) 405.
8 M.J. Frisch, H.F. Schaefer, III and J.S. Binkley, J. Phys. Chem., 89 (1985) 2192.
9 M. Scarlett and P.R. Taylor, Chem. Phys., 101 (1986) 17.
10 P.C. Burgers, J.L. Holmes and J.E. Szulejko, Int. J. Mass. Spectrom. Ion Processes, 57 (1984) 159.
11 P.C. Burgers, J.L. Holmes and A.A. Mommers, Int. J. Mass. Spectrom. Ion Processes, 54 (1983) 283.
12 G. Herzberg, Molecular Spectra and Molecular Structure, Vol. III, Van Nostrand, Princeton, 1967, p. 276.
13 J.C. Tully, in W.H. Miller (Ed.), Dynamics of Molecular Collisions, Part B, Plenum Press, New York, 1976, p. 217.
14 J.C. Lorquet and B. Leyh-Nihant, J. Phys. Chem., submitted for publication.
15 F. Remacle, D. Dehareng and J.C. Lorquet, J. Phys. Chem., submitted for publication.
16 J.H. Dunning, J. Chem. Phys., 53 (1970) 2823.
17 The program system ALCHEMY–MOLECULE incorporates the MOLECULE Gaussian integral program and the ALCHEMY SCF and CI wave function generator programs. MOLECULE was written by Dr. J. Almlöf of the University of Uppsala, Sweden. ALCHEMY was written at the IBM San José Research Laboratory. The interfacing of these programs was performed by P.S. Bagus. For a description of MOLECULE, see J. Almlöf, Proceedings of the Second Seminar on Computational Problems in Quantum Chemistry, Max Planck Institut, München, 1973, p. 14. For a description of ALCHEMY, see P.S. Bagus, in Selected Topics in Molecular Physics, Verlag Chemie, Weinheim, 1972, p. 187.
18 R. McWeeny, Mol. Phys., 28 (1974) 1273.
19 L. Salem, C. Leforestier, B. Segal and R. Wetmore, J. Am. Chem. Soc., 97 (1975) 479.
20 J. Lievin and G. Verhaegen, Theor. Chim. Acta, 42 (1976) 42.
21 C. Cohen-Tannoudji, B. Diu and F. Laloë, Mécanique Quantique, Vol. II, Hermann, Paris, 1973, Chap. XII.
22 L. Goodman and B.J. Laurenzi, Adv. Quantum Chem., 4 (1968) 153.
23 A.J. Lorquet, J.C. Lorquet, H. Wankenne and J. Momigny, J. Chem. Phys., 55 (1971) 4073.
24 S.P. McGlynn, T. Azumi and M. Kinoshita, Molecular Spectroscopy of the Triplet State, Prentice-Hall, Englewood Cliffs, 1969.

25 C.E. Moore, Atomic Energy Levels, NSRD-NBS 35, Vol. 1, 1971.
26 L. Landau and L. Lifshitz, Quantum Mechanics, Pergamon Press, London, 1958.
27 E.E. Nikitin, Chemische Elementarprozesse, Springer-Verlag, Berlin, 1968, p. 43.
28 J.B. Delos, J. Chem. Phys., 59 (1973) 2365.
29 W. Forst, Theory of Unimolecular Reactions, Academic Press, New York, 1973, Chap. 11.